

New Approach of Neural Network for Controlling Locomotion and Reflex of Humanoid Robot

Zaier Riadh and Kanda Shinji
Fujitsu Laboratories Limited
Japan

1. Introduction

In recent years, several humanoid robotic platforms have been developed, and most of them were dealing with hardware problems to closely replicate the appearance and the motion ability of human beings. Along with this, motion control also has been advanced, and much work has been focused on the dynamics of the robot using the zero moment point (ZMP) approach (e.g. Vukobratovic & Juricic, 1969; Miura & Shimoyama, 1984; Kajita & Matsumoto, 2001; Huang et al., 2001). Huang et al. proposed a method for planning a walking pattern, where the reference trajectory is designed offline for given constraints on the foot and ground, and satisfying a particular ZMP constraint using third order spline functions. More recently, biologically inspired control strategies have been proposed to generate autonomously adaptable rhythmic movement. These are based on a neuronal network, termed a central pattern generator (CPG) (e.g., Griller, 1985; Taga et al., 1991; Taga, 1995) that is capable of generating a rhythmic pattern of motor activity in the absence of sensory input signals. Taga et al. demonstrated that bipedal locomotion can be realized as a global limit cycle generated through entrainment between a neural network consisting of a neural oscillator and the physical system.

On the other hand, toward a safe interaction of the humanoid robot with the environment, Morisawa et al. presented a method to generate an emergency stop motion based on the evaluation on the ZMP and the center of gravity (COG). Okada et al. presented a motion emergency system based on attractor design of the nonlinear dynamical system. Huang et al. proposed a feedback sensory reflex, which consists of ZMP reflex, landing-phase reflex, and a body-posture reflex. However, in the presence of large disturbances, the ZMP will have an arbitrary location that can be out of the stable region in spite of the stability of the robot's upper body.

In this chapter, we deal with both the motion patterns generation and reflexes against sudden events. Instead of using complex modeling and dealing with highly non-linear equations (Okada et al., 2005; Huang & Nakamura, 2005), our control strategy in generating rhythmic motion is simply based on piecewise linear oscillators and a small number of easily tunable parameters. The method needs not to satisfy constraints on robot's foot or ZMP stability margin as in (Huang et al., 2001). It simply uses piecewise-linear functions

and first order low-pass filters generated by an original recurrent neural network (RNN) (Zaier & Nagashima, 2006), where the “integrate and fire” neuron model (Gerstner, 1995) has been used. The method, therefore, provides much flexibility to the pattern generator so that combination of reflexes during locomotion can be realized without complexity or re-design of the system.

To deal with sudden events and large disturbance acting on the robot, most recent works have been approaching this problem by proposing reflex action for each event separately (Huang & Nakamura, 2005; Zaier & Nagashima, 2006). In contrast, our approach consists of presenting the reflex system in a unifying form with regards to four types of sudden events, where we use a simple recognizer based on Bayes rule to detect unexpected events. In this research framework, we 1) add normal feedback signals when a relatively small disturbance is detected by the gyro sensor; 2) change the walk parameters such as the gait, the stride, or the walk posture; 3) add an extra motion at some joints besides the motion generator outputs; 4) stop the walk motion in the case of large disturbance and generate a reflex based on the sensory data and an interpolation of four predefined postures. It should be noticed that the reflexes in 1) and 4) are decided according to the robot’s upper body oscillation rather than the ZMP stability margin (Huang & Nakamura, 2005). Moreover, since the leg during swing phase is made very compliant, there will be neither tipping over when landing nor colliding with an obstacle.

In this chapter, we consider more focus on the reflex against sudden obstacle from the stability point of view. Indeed, the behavior of the robot when it encounters an obstacle depends on the timing and location of the collision with regards to the sole plate under the robot leg. In other words, and by considering the state space diagram, the stability of the robot will depend on the distance of the robot state from the equilibrium point and the ability of the robot to return to that point. In this research framework, therefore, the primitive reflex against sudden obstacle that has been proposed in (Zaier & Nagashima, 2006) will be modified by processing the force sensors’ outputs such that the generated reflex movement can smoothly shift the robot state to the attraction domain of the equilibrium point.

Experiments using Fujitsu’s humanoid robot HOAP-3 (Murase et al., 2001; Fujitsu Automation Ltd.) demonstrate that the reflex movement is successfully integrated with the rhythmic motion. The robot robustly walks on a number of different ground surfaces and exhibits an efficient natural looking reflex mode.

2. Neural network of rhythmic motion and reflex

Shaping an arbitrary motion pattern takes effort to think about the functions that fit the desired task with regards to given constraints. On the other hand, continuous piecewise linear functions have proved to be very powerful tools in modeling and analyzing nonlinear systems. For instance, to fit the real dynamics of the robot, the profile of the rolling motion of a humanoid robot can be approximated using (1).

$$\varepsilon_i \frac{da(t)}{dt} + a(t) = c(t), \quad (1)$$

where $c(t)$ is the input signal described as a piecewise linear function in time t , $a(t)$ is the activation function. In fact, for small oscillations the passive behavior fits a sine-wave. But,

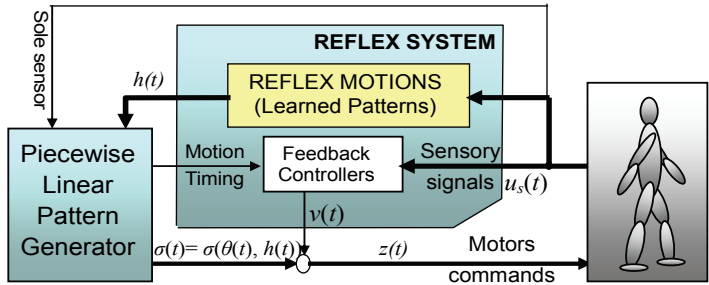


Fig. 1. Overall scheme of the reflex system and motion pattern generator

in general, the trajectories for the biped joints are not sine functions with only one frequency component. For such situations, a combination of more primitive functions will be much interesting. The input signal $c(t)$ can be expressed as time series of N piecewise-linear functions $u_i(t)$:

$$c(t) = \sum_{i=1}^N c_i u_i(t - t_i), \tag{2}$$

where $u_i(t) \in [0,1]$, $t_i \geq 0$ and c_i is a real number.

Let's write the equations of the proposed recurrent neural network (Fig.1) that controls the movement of the humanoid robot as follows;

$$\frac{d\theta_i(t)}{dt} = f_i(t, \theta_i) \tag{3}$$

$$f_i(t, \theta_i) = -\frac{1}{\varepsilon} \theta_i(t) + g_i(t) \tag{4}$$

where the index i represents either rolling or pitching, θ_i is the generated motion to the joints, $f_i(t, \theta_i)$ is a piecewise continuous function in time t , $g_i(t)$ is a piecewise function generating the walking as in (2). At the equilibrium points the robot is controlled by the following PD controller,

$$\begin{cases} \frac{dx_i}{dt} = -a_{ii}x_i + \sum_{j=1, j \neq i}^N \frac{a_{ij}}{a_{ii}}x_j + \frac{b_i}{a_{ii}}u_s \\ v(t) = \sum_{i=1}^N c_i x_i(t) \end{cases} \tag{5}$$

where $v(t)$ is the controller's output to the pitching or rolling joints, u_s is the sensory input, N is the order of controller. In this research framework we limit $N=2$ as it reduces the controller to two coupled neurons (Zaier & Nagashima, 2006). The parameters $a_{ii} > 0$, a_{ij} , and b_i can be easily designed, since optimal values are not required in the proposed design approach. Therefore, the motors' commands can be expressed as follows;

$$z_i(t) = v(t) + \sigma(\theta_i(t), h_i(t)), \tag{6}$$

where $h_i(t)$ represents the reflex motion, and $z_i(t)$ is the motor commands.

Note that the solution of (3) is $\theta_i(t) = \theta_{i0}(t) + \int_{t_0}^t f_i(s, \theta_i) ds$, and since $g_i(t)$ is a piecewise continuous in t and satisfies the Lipschitz condition over the interval $[t_0, t_1]$ (time interval

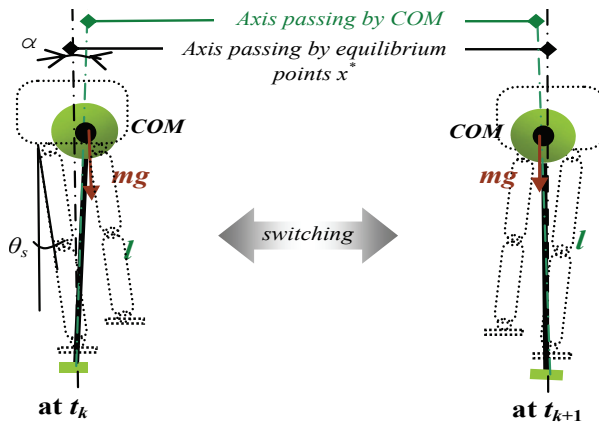


Fig. 2. Commutation of the robot state between equilibrium points defined at the single support phase

during commutation between single support phases), then $f_i(t, \theta_i)$ satisfies a local Lipschitz condition over the interval $[t_0, t_1]$ and has a unique solution (Khalil, 1996).

3. Generation of walking motion pattern

3.1 Stability at the single support phase

While the inverted pendulum model considerably simplifies the control of the humanoid robot, the inertia effect of distributed masses such as the arms may present a limitation to that approach. Our method, although inspired by the inverted pendulum, it considers not strictly the system dynamics. In other words, the method can generate a rhythmic movement without solving the nonlinear differential equations of the system dynamics. To illustrate the idea, consider Fig.2, where continuous commutations between single support phases take place. Let's model the system by a second order ODE with a feedback control input as follows;

$$\frac{d^2\alpha}{dt^2} + 2\zeta \frac{d\alpha}{dt} - \mu\alpha = u_g(\alpha), \tag{7}$$

where $\alpha \in \mathbb{R}$ is the counter clockwise angle of the inverted pendulum from the vertical, $\zeta \in \mathbb{R}$ is damping ratio, $\mu = g/l \in \mathbb{R}$, and $u_g \in \mathbb{R}$ is the feedback control input stabilizing the system. Let $\alpha = \theta - \theta_s$, where θ is the angular position of the hip joint and θ_s is its value when the projection of the centre of mass (COM) is in the support polygon. Then (7) can be rewritten as follows;

$$\frac{d^2\theta}{dt^2} + 2\zeta \frac{d\theta}{dt} - \mu\theta = u_g(\theta), \tag{8}$$

where $u_g(\theta)$ is the gyro feedback signal stabilizing the inverted pendulum around $\theta = \theta_s$. Then at each equilibrium point the system has the same eigenvalues as follows;

$$\lambda_{1,2} = -\zeta \pm \sqrt{\zeta^2 + \mu} \tag{9}$$

Since $\zeta \ll \mu$, the equilibrium points (9) are saddle ones. Therefore, to generate periodic movement as explained in Fig. 2, we must first stabilize the equilibrium points by a feedback control $u_g(\theta) = k_1\theta + 2k_2d\theta/dt$ using the measured angular velocity of the inverted

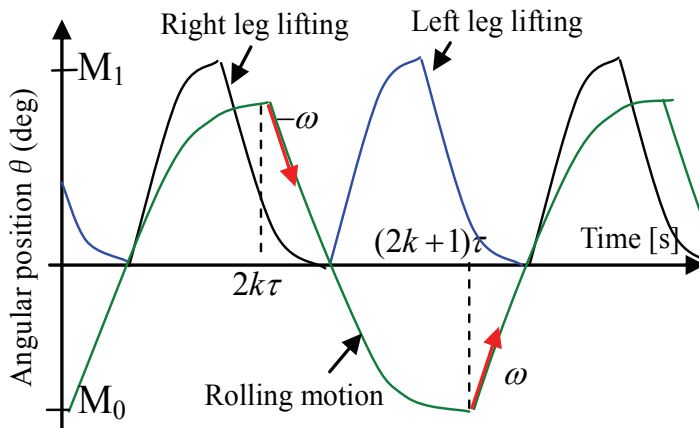


Fig. 3. The position commands to the joints; rolling commands to the ankle and hip, lifting commands to the ankle, knee and ankle joints, where the commands to the knee is twice of the ankle with opposed sign.

pendulum. It should be noted that our approach is based on rough model of the robot; there is no need to design optimal feedback gain, however, this gain has to be decided not to cause high vibration of the robot mechanism.

3.2 Rolling motion

The rhythmic motion is generated with regards to the rolling profile that is approximated as trapezoidal form, and smoothed using (1). The position command to the hip and ankle is illustrated by Fig.3. The control law at the switching times $t = k\tau$ is expressed as follows;

$$\begin{cases} \theta(t^-) = (-1)^{k+1} \theta_{\max}, & d\theta/dt|_{t=t^-} = 0 \\ \theta(t^+) = (-1)^{k+1} \theta_{\max}, & d\theta/dt|_{t=t^+} = (-1)^k \omega \end{cases} \quad k = 1,2,3\dots \quad (10)$$

where k is the number of half walking cycle τ , the t^- and t^+ are the times just before and after commutation, respectively. For $t \neq k\tau$ the state trajectory will follow the desired rolling profile as described in Fig. 3, and the stability of the equilibrium points is guaranteed by the gyro feedback loop added to the system as in (8).

Let's formulate the rolling motion $\theta(t)$ during commutation from M_0 to M_1 as a function of time delay ε , joint angular velocity ω , walking cycle T , and the rolling amplitude a_s .

$$\theta = f(\varepsilon, \omega, T, \theta_s), \quad (11)$$

and define the operator $u(\cdot)$ such that $u(t_i, \omega_i) = \omega_i(t-t_i)$ with $0 \leq u(t_i, \omega_i) \leq 1$. Using this operator, the periodic rolling motion can be expressed as follows;

$$\varepsilon \frac{d\theta(t)}{dt} + \theta(t) = \theta_s [u(t_{r0}, 2\omega_r) - 2u(t_{r0} + (n + f_1)T, \omega_r) + 2u(t_{r0} + (n + f_2)T, \omega_r) - u(t_f, 2\omega_r)], \quad (12)$$

where t_{r0} , t_f are the switching times for the start and end of the rolling motion, respectively, and n is the number of walking steps. The f_1 and f_2 are the relative times with regards to the gait. By letting $p = t_{r1} - t_{r0} - 1/\omega_r$ be the time during which the robot stays at the maximum rolling and t_{r1} be the first switching time at the single support phase, we can write $f_1 = (1/\omega_r + p)/T$ and $f_2 = 2f_1 + 1/(\omega_r T)$.

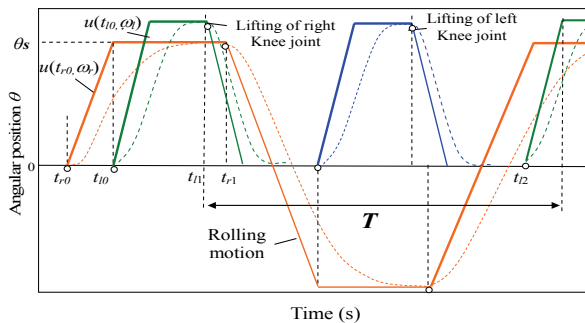


Fig. 4. Rolling motion pattern and design parameters.

The commands $\theta_{am}^r(t)$ and $\theta_{hm}^r(t)$ will be sent respectively to the hip and ankle joints, which are given by,

$$\theta_{am}^r(t) = -\theta_{hm}^r(t) = \theta(t) + \theta_{fb}^r(t), \tag{13}$$

where $\theta_{fb}^r(t)$ is the feedback signal stabilizing (8).

Since the position command to the hip is the same as that to the ankle joint with opposed sign, the robot upper body orientation in the absence of disturbance remains unchanged, in other words the angular velocity around the rolling axis during locomotion is zero. Notice that the control law described by (10) is explicit of time. Instead, the state commutation can be constrained by angular velocity $d\theta/dt=0$, and the control law becomes independent of the cycle time as a pure feedback law, however, the commutation time will be no more constant.

3.3 Swing motion

The dynamic of the swing leg can be considered the same as that of a pendulum, and hence it is inherently stable without any compensator. This motion is generated in a similar fashion as that of the rolling motion, and according to Fig. 4 it is expressed by the following equation;

$$\varepsilon \frac{d\theta_l(t)}{dt} + \theta_l(t) = a_l [u(t_{l0}, \omega_l) - u(t_{l1} + nT, \omega_l) + u(t_{l2} + nT, \omega_l) - u(t_{lf}, \omega_l)], \tag{14}$$

where θ_l is the lifting motion and a_l is its amplitude. The t_{l0} and t_{l2} are the switching times of lifting for the first and second half walking cycle, t_{l1} and t_{lf} are the switching times of landing for the first and the last half cycle, and ω_l is the joints' angular velocity. It should be noticed that the proposed motion pattern generator generates dynamic walking motion as shown in Fig. 3, where the lifting time t_{l0} in Fig. 4 is very close to the rolling time t_{r0} . Similarly, the angular position θ_s generating the stride is expressed by the following equation;

$$\varepsilon \frac{d\theta_s(t)}{dt} + \theta_s(t) = a_s [u(t_{s1} + nT, \omega_s) - u(t_{s2} + nT, \omega_s)], \tag{15}$$

where a_s is the amplitude of the angular position generating the stride. The ω_s is the joints' angular velocity. The t_{s1} and t_{s2} are the times at the start and the end of stride, respectively. On the other hand, we assume that the landing of each leg is accomplished with a flat foot on a flat ground, and the thigh and shank of the robot have the same length. Therefore, with respect to the angles defined by (Fujitsu Automation Ltd.), this condition can be satisfied as follows.

$$\begin{cases} \theta_{am}^p(t) = \theta_l(t) + \theta_{fb}^l(t) + \theta_s(t) \\ \theta_{km}(t) = -2\theta_l(t) \\ \theta_{hm}^p(t) = \theta_l(t) + \theta_{fb}^l(t) - \theta_s(t) \end{cases}, \quad (16)$$

where θ_{am}^p , θ_{km} , and θ_{hm}^p are the pitching motor commands to the ankle, the knee and the hip, respectively. The $\theta_{fb}^l(t)$ is the feedback signal to the ankle and the hip, satisfying the stability of inverted pendulum in the sagittal plane as in (7).

Moreover, to minimize the force of the collision of the landing leg with the ground, instead of using impact model, besides (17), we control the damping factor b_s and the spring stiffness k_s of the virtual damper-spring system (19) such that the leg is very compliant at the swing phase, and gradually get stiffer till it reaches the maximum stiffness at the single support phase.

$$m \frac{d^2 y_c(t)}{dt^2} + b_s \frac{dy_c(t)}{dt} + k_s y_c(t) = F_y, \quad (17)$$

where $y_c(t)$ is the displacement of the mass m along the vertical axis, and F_y is the external force acting on the supporting leg. The angular positions to the motors' commands becomes

$$\begin{cases} \theta_{am}^p(t) = \theta_l(t) + \theta_s(t) + \theta_{fb}^l(t) + \theta_c(t) \\ \theta_{km}(t) = -2\theta_l(t) - 2\theta_c(t) \\ \theta_{hm}^p(t) = \theta_l(t) - \theta_s(t) + \theta_{fb}^l(t) + \theta_c(t) \end{cases}, \quad (18)$$

where $\theta_c(t) = \arcsin(y_c(t)/L)$ is the angular position induced by the virtual damper spring system in (17), and L is the length of the thigh.

4. Reflex system

In order to prevent the falling down of a humanoid robot when it suffers a sudden deviation from its stable state, we have proposed a reflex system that can be triggered by sensory signals. In the previous result (Zaier & Nagashima, 2006), we studied three cases of sudden events; (1) when there is a sudden change in the ground level, (2) when the robot is pushed from arbitrary direction, and (3) when there is a sudden change in load.

4.1 Reflex against large disturbance

For the case of large disturbance, we defined a normalized angular velocity at the x-y plane termed gyro index "gi", and it is given by,

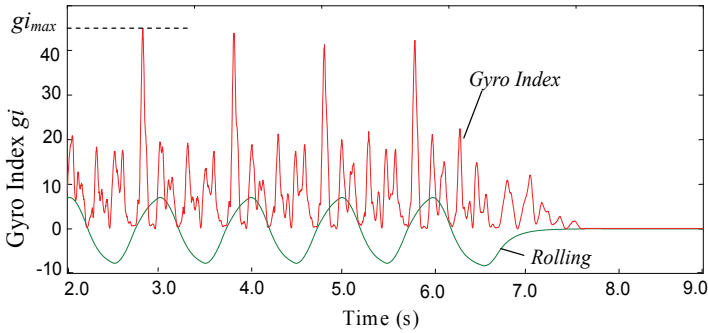


Fig. 5. Gyro index and rolling joint’s output during walking when no large disturbance is present

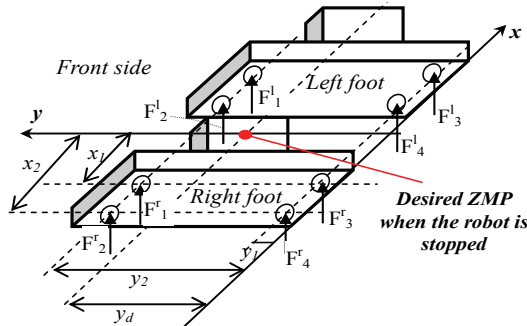


Fig. 6. Sole reaction forces acting on the sole plate and desired ZMP.

$$g_i = \sqrt{\mu^2 gyro_y^2 + gyro_x^2} , \tag{19}$$

where $gyro_x$ and $gyro_y$ are the components of the gyro sensor’s output along the rolling and pitching axis, respectively. The parameter $\mu=L/w$ is the size ratio of the sole plate, where L and w are the length and the width of the robot sole plate, respectively. The decision about the presence of large disturbance is based on a threshold Tg_i , which we obtained experimentally by disturbing the robot to the level beyond which stability by PD controllers will not be possible. Fig. 5 shows the experimental result of the *Gyro index* in the absence of large disturbance. Moreover, we defined four postures around the walking motion which we called learned postures. When a large perturbation occurs such that the threshold Tg_i is touched, the robot will stop walking and shifts its pose to one of learned postures selected according to the measured ZMP position. A gyro feedback controller will be activated stabilizing the final pose the humanoid robot has shifted to. In order to find the ZMP during locomotion, we simply use the sole reaction forces defined in Fig. 6, which is calculated using the force sensors’ values as follows,

$$x_m = [x_1(F_1^r + F_3^r - F_2^l - F_4^l) + x_2(F_2^r + F_4^r - F_1^l - F_3^l)] / F_T \tag{20}$$

$$y_m = [y_1(F_3^r + F_4^r + F_3^l + F_4^l) + y_2(F_1^r + F_2^r + F_1^l + F_2^l)] / F_T, \tag{21}$$

where F_T is the sum of all forces acting on the legs. Notice that the stride effect on y_m is neglected since the duration of the double support phase is almost zero and is much smaller

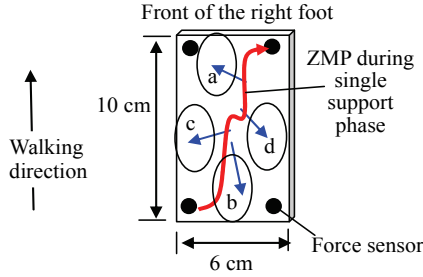


Fig. 7. Sole plate of the robot; the curve in red is the ZMP trajectory during the single support phase. The (a, b, c, and d) are the zones to which the ZMP will shift when disturbances occur

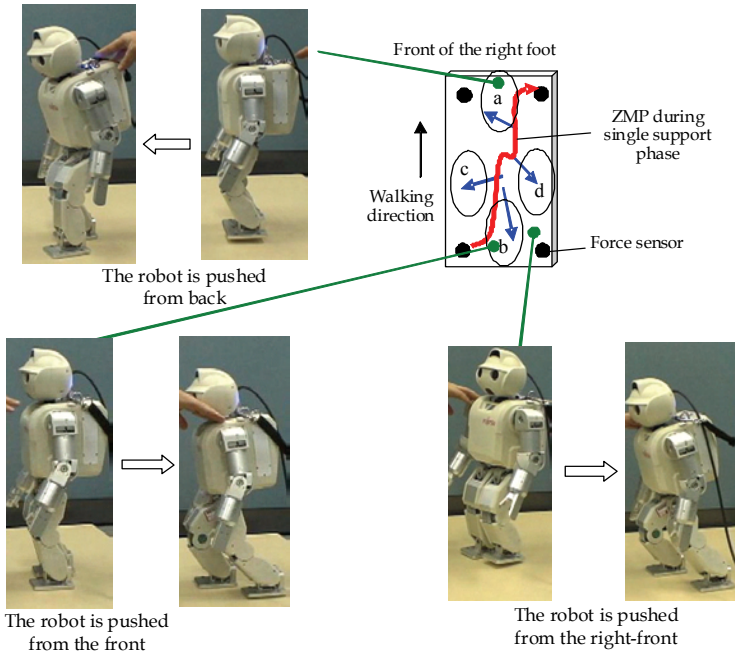


Fig. 8 Defined zones (a, b, c, and d) under the sole plate and reflex actions that take place when the large disturbance occurs. The reflex consists of switching the pose of the robot to the appropriate predefined posture according to the ZMP position. Notice that when the robot is pushed from the right-front, the ZMP position is between zone (b) and zone (d) shown in Fig 7, and consequently the left leg is stepped back to the left side.

than the time delay of the ZMP controller. The ZMP during walking and in the absence of large disturbance can be described by the curve in Fig.7. To generate a reflex motion when large disturbance acts on the robot's upper body, we define four zones under the sole plate and for each zone we define a posture such that when the ZMP is shifted to one zone in the presence of large disturbance, the robot will stop walking and modifies its pose to the appropriate posture, as described in Fig. 8. If the ZMP shifts between two of these four zones, linear interpolation will be considered between the two corresponding defined postures. Notice that a large disturbance is detected when the gyro index (19) touches the

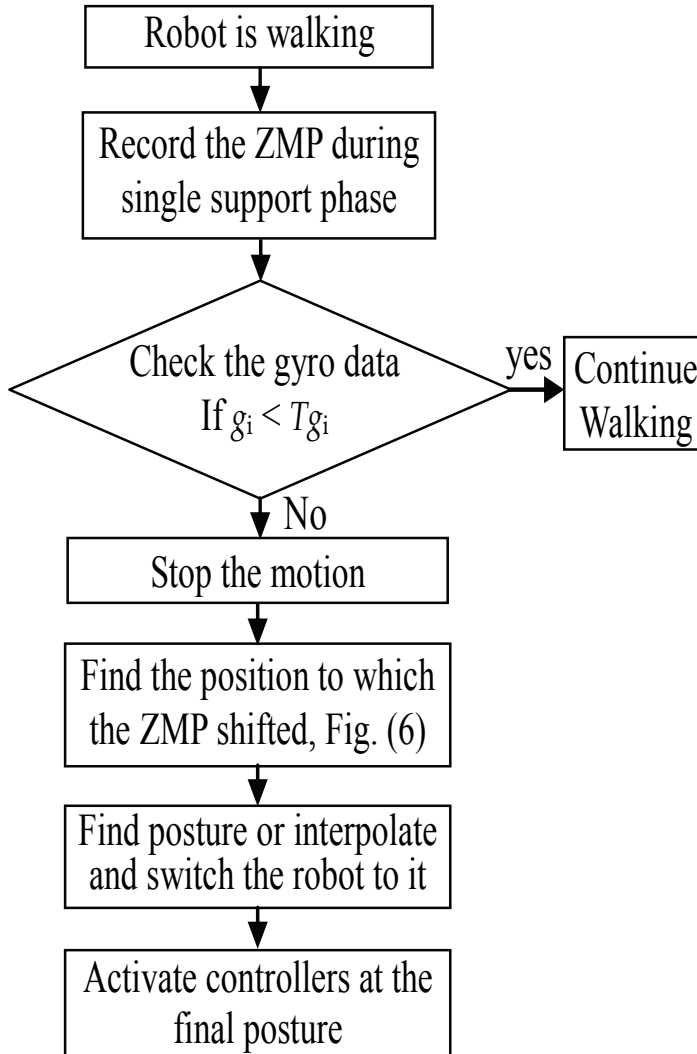


Fig. 9. Flowchart of reflex activation when a large disturbance is present

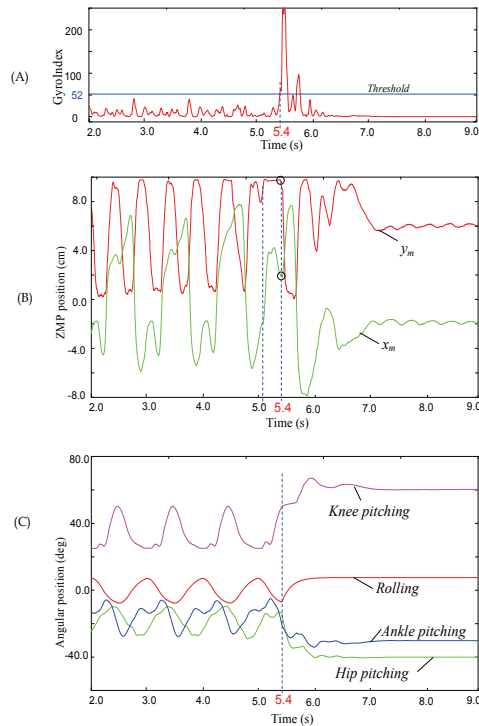


Fig. 10. Detailed results in the presence of large disturbance; (A) shows the gyro index that touches the threshold at 5.4 s. (B) shows the ZMP positions during walking defined within the support polygon, where x_m is varying between the right and left legs, while y_m is defined along the sole plate from 0 to 10 cm. At 5.4 s the large disturbance was detected and the ZMP has shifted to the circled points, which correspond to $x_m = 2.0$ cm and $y_m = 8.4$ cm. Finally, (C) shows the pitching and rolling joints' outputs of the left leg.

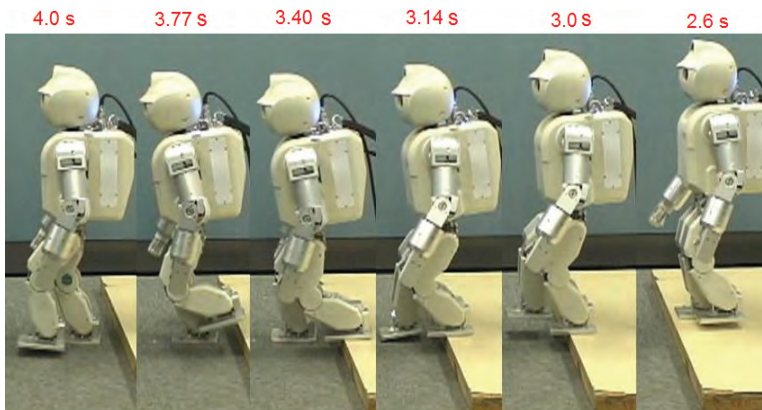


Fig. 11. HOAP-3 walking and encountering a sudden change in ground level

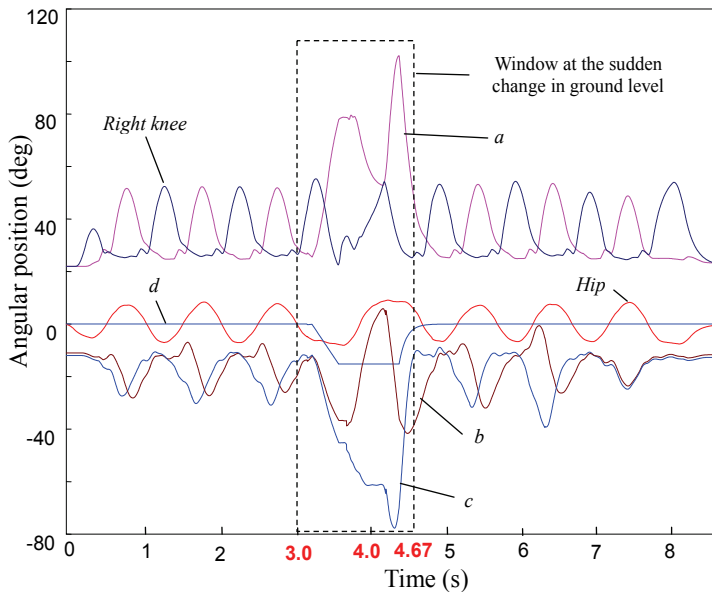


Fig. 12. Joints outputs at the sudden change in ground level. Pitching of the knee (*a*), ankle (*b*), and hip (*c*) joints of the left leg. (*d*): Extra motion added to the pitching joints of supporting leg

threshold T_{gi} . The steps from the detection of large disturbance till the activation of a reflex motion are described by the flowchart in Fig. 9. The experimental results of the case when the robot is pushed from the back are detailed in Fig. 10.

4.2 Reflex against sudden change in ground level

Other type of sudden event we studied is the reflex against sudden change in ground level (Fig. 11) that is detected using a photo-interrupter attached to the front of the robot foot. The reflex movement will be triggered when the photo-interrupter, at the landing time of the leg, does not detect a ground. The reflex movement consists of increasing the stride so that the foot collides not with the upper ground. Afterwards, the supporting leg will be contracted in height till the swing leg touches the lower surface. After landing, the walk parameters (gait and stride) will be set to their previous values. Notice that our proposed reflex needs not to know about the ground elevation. This parameter is detected automatically by the sole sensor, where we assume that the change in the ground level is within the hardware limit of the robot. The joints' outputs are shown in Fig. 12. The extra motion (*d*) is added to the supporting leg joints contracting the leg at height. The contraction is stopped when the swing leg touches the lower surface. The contraction phase of the supporting leg starts when the linear velocity of the upper body is almost zero. Moreover, the contraction speed is low enough to ensure that the contracting leg will not affect the stability of the robot. The walking cycle time is augmented by about 50% at the sudden change in ground level. The motion of the supporting leg is modified accordingly.

4.3 Reflex against sudden obstacle

This type of reflex is activated when a sudden obstacle touches the sole sensor of the leg at the swing phase. We assume here that the foot of the leg remains parallel to the ground during the swing motion, which is satisfied by (16).

The reflex process is abstracted as follows:

- Detect the sudden obstacle with a sole sensor.
- Stop the motion of the robot.
- Move the state of the robot to the attraction domain of the stable equilibrium point.
- Resume the walking motion with negative stride, then follow upper level control.

Let's write the equations of the reflex motion as follows,

$$\varepsilon_p \frac{dh_p(t)}{dt} + h_p(t) = u(t - t_{sw})(a_l - \theta_{swp}) \quad (22)$$

$$\varepsilon_r \frac{dh_r(t)}{dt} + h_r(t) = u(t - t_{sw})(\theta_s - \theta_{swr}) \quad (23)$$

where $u(t_i)$ is a unit step function starting at t_i . The $h_r(t)$ is the angle to the pitching joints of the leg touching the obstacle, which will be added as θ_l in (16), and $h_p(t)$ is the angle to the rolling joints of the ankles and hip of both legs. The ε_r and ε_p are neurons' time delays with much smaller values than ε in (4), θ_{swr} and θ_{swp} are the rolling and pitching values, respectively, at the time t_{sw} , when the sudden obstacle is detected, a_l is defined in (14), and θ_s is the rolling amplitude. Fig. 13 shows HOAP-3 detects a sudden obstacle as it walks. The joints' outputs are shown in Fig. 14. At 3.0 s, the sole sensor of the left leg touches the obstacle and the robot stops landing its leg and increases its rolling motion while keeping the gyro feedback controller active. The robot, then, retracts the left leg to its previous landing position. This is shown in Fig. 14 by the pitching motion of the hip, knee, and ankle within the time interval [3.0s, 4.8s]. The walking is resumed successfully at 6.8 s. Notice that the leg during swing motion is made very compliant, where the stiffness is controlled during the gait such that the leg at the middle of the supporting phase is very stiff, while it is very compliant during the swing phase.

4.4 Reflex against sudden change in load

We consider the reflex when the humanoid robot detects a sudden change in load as it walks, which is considered as a large disturbance but to the level that the ZMP remains

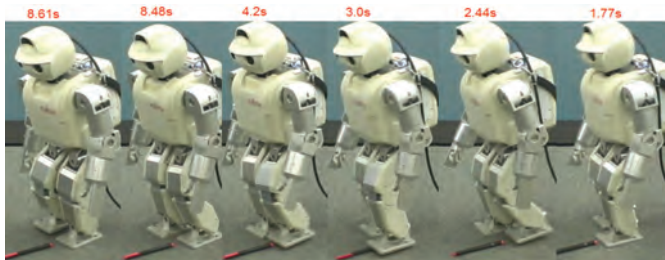


Fig. 13. Reflex against a sudden obstacle while walking.

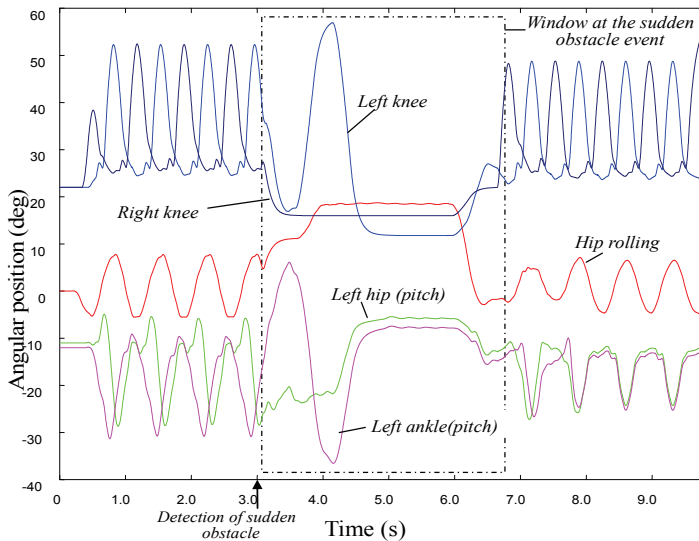


Fig. 14. Joints outputs when reflex against sudden obstacle is activated

inside the support polygon. The proposed reflex policy is shown in Figs. 15 and Fig. 16. The reflex motions θ_w and θ_a will be generated simultaneously at the ankles and waist joints, respectively (Fig. 15 c). The amplitudes of these angles are set according to the deviation angle of the upper body. During this phase only, the gain of the gyro feedback controller, which works against oscillation of the robot's upper body, is reduced by more than half. After this phase, the gain of the gyro feedback controller is set to its previous value (Fig 15 d). Fig. 17 shows HOAP-3 carrying a relatively heavy box. As it walked, the box was taken away and the robot could walk stably and compensate for the change by adjusting its walking posture at the ankle and waist joints according to the algorithm in Fig. 16. The positions of the ankles and their change during walking are shown in Fig. 18. The reflex motion is generated within the time interval [6.0s, 7.0s]. It should be noticed here that the reflex is triggered by the gyro sensor when its value exceed a given threshold, while the reflex motion is selected according to the recorded ZMP at the disturbance detection time.

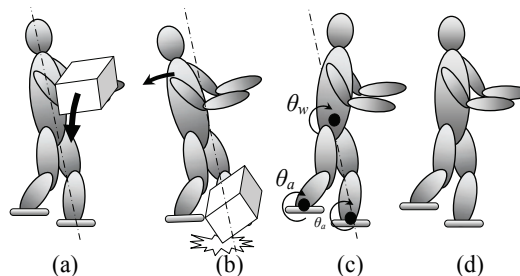


Fig. 15. Proposed control policy at a sudden change in load; (a) The robot is carrying a box, (b) The box is fallen down, (c) generation of reflex motion in the waist and ankle joints, (d) ZMP and Gyro feedback control.

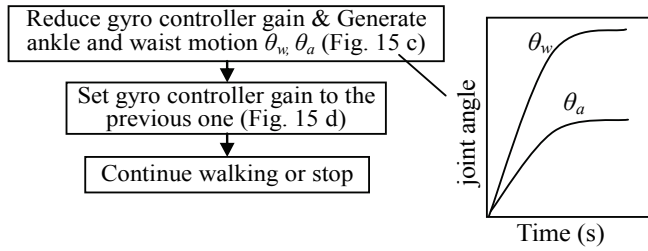


Fig. 16. Flowchart of reflex at sudden change in load.

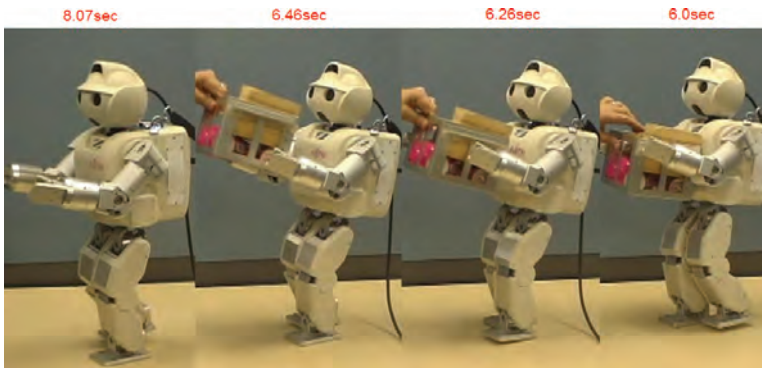


Fig. 17. Reflex against sudden change in load while walking

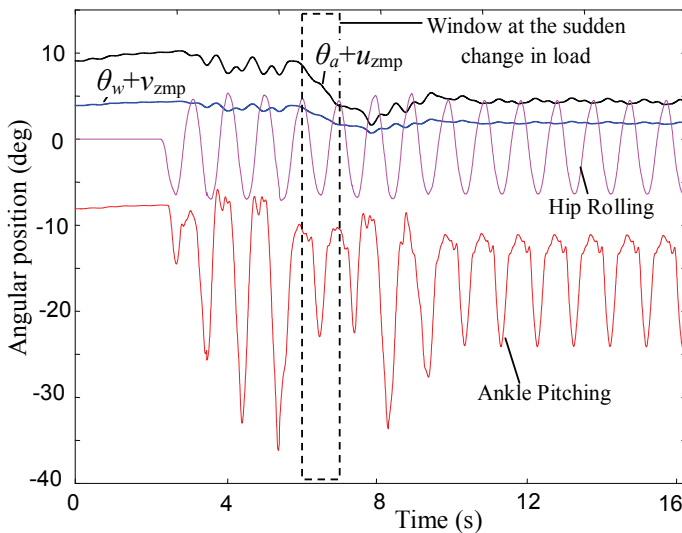


Fig. 18. Joints outputs at the sudden change in load. As shown in Fig. 16, θ_a , and θ_w are the angles added to the ankle and waist joints, respectively. u_{zmp} , and v_{zmp} are the ZMP feedback controls to the ankles and waist joints.

4.5 Unified reflex system

To deal simultaneously with several types of undesired events, the reflex system has to be designed with a structure that can be extended to cover, to some extent (e.g., hardware), several types of sudden events that may act on the robot. If we consider that prior knowledge about the type of sudden event is provided, and by defining a discriminant function $d_i(s)$ based on the Bayes rule, the general structure of the recognizer can be represented as shown in Fig. 19. In this research frame work, the recognizer is limited to four types of sudden events that we studied in the previous subsection. To build up the recognizer, sensory data and motion related parameters are collected. When extracting the appropriate features required for each type of sudden event, we realized that the recognizer can be simplified into two dichotomizers (Fig. 20). The first dichotomizer consists of reflex actions against large disturbances. That is, when an input from the gyro sensor s_1 exceeds a given threshold, discriminant functions d_1 and d_2 will use that feature but the decision will depend on input's feature s_2 . For instance, when the ZMP remains inside the support polygon, the disturbance is considered to be of type one. If the ZMP leaves the support polygon, then a disturbance will be of type two. For example, pushing a robot as it is walking can be classified as a large disturbance of type one if the ZMP remains inside the supporting polygon, otherwise, it is of type two. As for the second dichotomizer, $d_3(s)$ activates the reflex action against a sudden change in ground level when the photo-interrupter that is attached to the front of the leg is enabled at landing time, while $d_4(s)$ activates the reflex against a sudden obstacle when the sole sensor of the swing leg touches an obstacle. Fig.21 shows the overall scheme of the reflex system and motion pattern generator.

4.6 Adaptive reflex system

In the previous subsection, although the reflex was proposed in a unified fashion with respect to four types of sudden events, adaptation of the reflex was not considered. For instance, the reflex against sudden obstacle, in some situation, may fail to prevent the falling

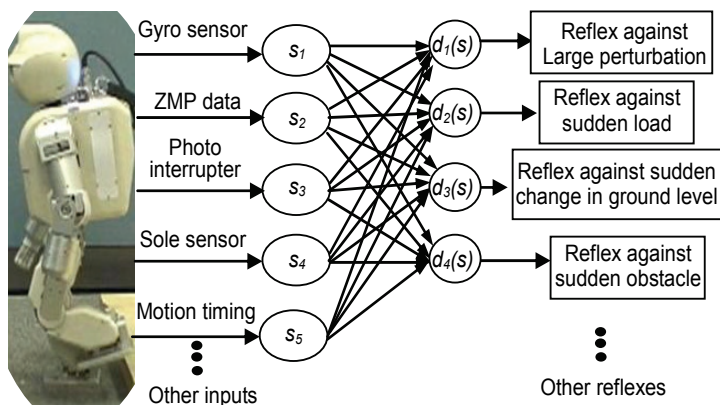


Fig. 19. General structure of the unexpected pattern recognizer, where s_i represents the normalized input signal and $d_i(s)$ is the discriminant function.

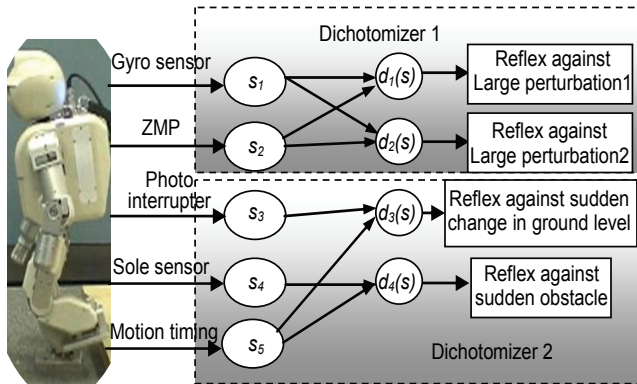


Fig. 20. Structure of the unexpected pattern recognizer after features extraction.

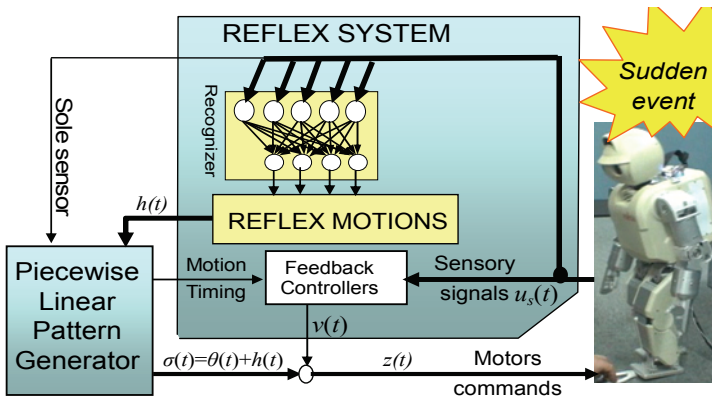


Fig. 21. Overall scheme of the reflex system and motion pattern generator; $\sigma(t)$ is the sum of reflex $h(t)$ and the motion pattern generator output $\theta(t)$

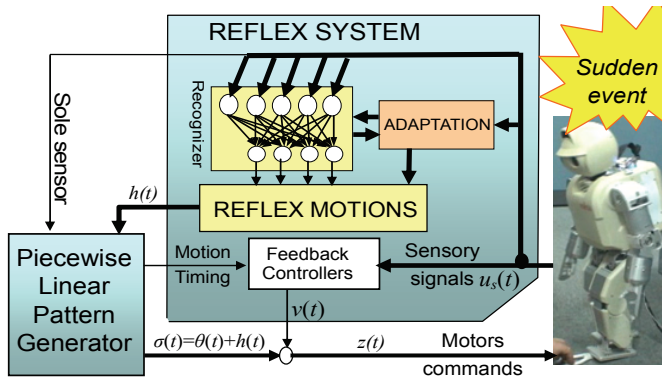


Fig. 22. Overall scheme of the adaptive reflex system and motion pattern generator

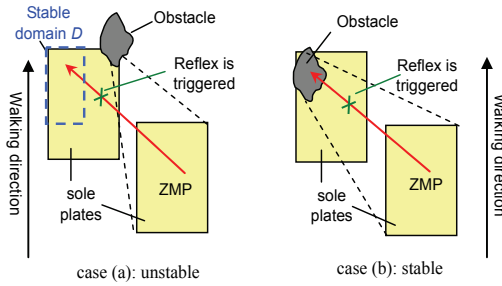


Fig. 23. The state of the robot depends on the relative position of the sudden obstacle with regards to the sole plate. Notice that the commutation of the state between equilibrium points is realised by gravity

of the robot. In this section, therefore, we propose a new adaptation algorithm as shown in Fig. 22, which will adapt the reflex motion and the recognizer as well. In this research framework we limit the adaptation to the reflex against sudden obstacle.

Let consider our previously proposed reflex (22) and (23) as a primitive one, and abstracted as follows:

- Detect the sudden obstacle with a sole sensor.
- Stop the motion of the robot.
- Move the state of the robot to the attraction domain of the previous equilibrium point.

However, if the obstacle does not provide a stable supporting surface, it will be hard for the robot to step forward and stand up stably on the obstacle. For instance, when an obstacle touches the obstacle in the half sole plate adjacent with the other leg, the robot state will not be able to return to the equilibrium point defined by the other leg.

Due to the dynamic walking pattern (i.e., the commutation of the ZMP from one leg to the other is realized by a free fall of the humanoid robot) and the presence of time delay in triggering the reflex, the ZMP may become out of the support polygon formed by the leg's sole plate and the obstacle (Fig. 23a), which make the primitive reflex unable to prevent the falling down of the robot. To face such a problem there are two solutions; either to increase the support polygon area or to change the robot posture so that the ZMP becomes inside the stability zone. Intuitively, it is easier to consider the first possibility rather than the second one, by rolling or pitching the ankle joint of the leg touching the obstacle. Moreover, using

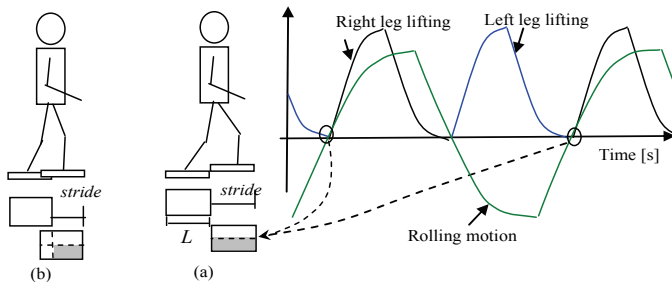


Fig. 24. The stability zone D is coloured in gray; it corresponds to the zone from which the landing and rolling to the other leg start

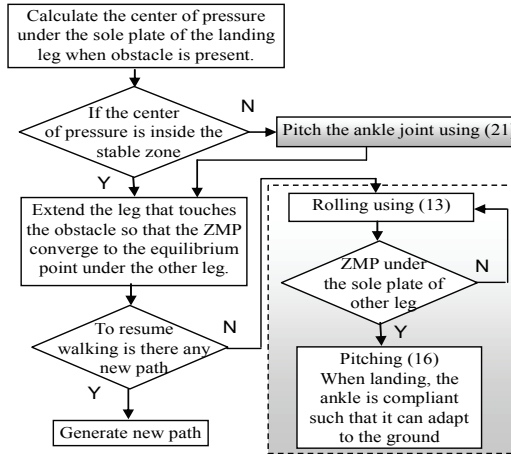


Fig. 25. Flowchart of the improved reflex against sudden obstacle, where the reflex is triggered when the sole plate touches the obstacle at the swing phase

dynamics calculation, it is possible to show that this reflex corresponds to the minimum energy the robot may spend to achieve stability. In some cases, however, environmental constraints may impose the second solution to be adopted, for instance, by lowering the COM, or even by relying on a fixed object nearby the robot. These intuitive actions can be considered as hints to adapt the neural network with additional reflexes covering cases similar to that of Fig.23a, which depend on the relative position of the obstacle with respect to sole plate and the environment surrounding the robot as well. Therefore, the augmented reflex is proposed as follows;

$$\begin{cases} \varepsilon_r \frac{ds_a}{dt} + s_a = s_a(t)u(t_{obs}) + k(u(t_{obs}) - u(t_{cont})) \\ \frac{dx_i}{dt} = -a_{ii}x_i + \sum_{j=1, j \neq i}^N \frac{a_{ij}}{a_{ii}}x_j + \frac{b_i}{a_{ii}}e_j(t) \\ r_a(t) = s_a(t) + \sum_{i=1}^N c_i x_i \end{cases}, \tag{24}$$

1.0 s
0.86 s
0.46 s
0.13 s
0 s

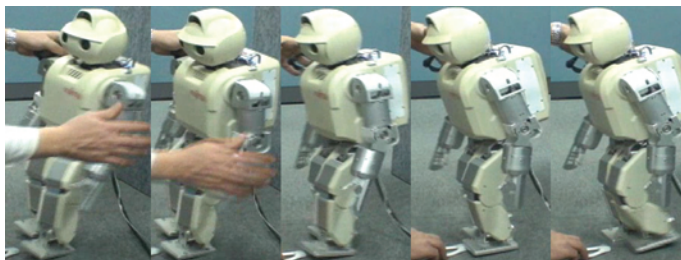


Fig. 26. Primitive reflex against a sudden obstacle while walking; the ZMP is outside the support polygon formed by the right leg and the obstacle.

where $u(t_i)$ is as defined in (22), $\epsilon_r > 0$, e_j is the distance of the ZMP from the center of the sole plate, k is the integration constant, $r_a(t)$ is the reflex motion to the ankle pitching joint. $s_a(t)$ is an integrated angular position from the time when the obstacle is detected (t_{obst}) till the time when the sole plate touches the ground making a stable support polygon (t_{cont}). The $a_{ii} > 0$, a_{ij} and b_i are parameters of the PD controller defined as in (5). The stability zone D is described in Fig. 24, which depends on the walking stride and is defined by the timing when the leg touches the ground (for dynamic walking the rolling at this timing is zero). Fig.25 shows the proposed adaptive reflex algorithm. Notice that the whole control diagram is shown in Fig. 22, where the adaptation part consists of (24) and some check regarding the stability domain D at the collision time. The first step consists of finding the center of pressure (or position of the obstacle). Then, if this position belongs to the stability zone D , the leg will expand in length by inverting the sign of sensor feedback output in (16) so that the state of the robot reaches the attraction domain of the equilibrium point under the supporting leg. Otherwise, the reflex (24) will be generated, which consists of augmenting the support polygon by pitching the ankle joint. Once the robot reaches the stable state it follows upper level commands, either by walking over the obstacle or stepping back and finding a new path. In the case of walking over the obstacle, the locomotion controller will generate a static walking; this is by shifting the time t_{10} from t_{r0} (Fig.4), so that the lifting starts only when the projection of COM is under the other leg. This walking style is also adopted by human whenever he walks on rough or unstable terrain.

Remark: The advantage of (24) over the pitching expression (22) is that only the ankle of the leg that collides with the obstacle is pitched by an angle such that the support polygon covers the ZMP at the collision time. Moreover, although we used a ZMP feedback loop besides (22), the response is not fast enough to prevent the falling down of the robot.

To show the effectiveness of our newly developed adaptive reflex we conducted two experiments. Fig. 26 shows the experiment results when HOAP-3 detects a sudden obstacle as it walks, using the primitive reflex. Since the collision position of obstacle with the sole plate is out of the stability zone D (Fig. 24), the robot was not able to get stable by the primitive reflex (22) and (23), and therefore it has fallen down. Fig.27 shows the case when the proposed reflex was implemented, where the joints' outputs are shown in Fig. 28.

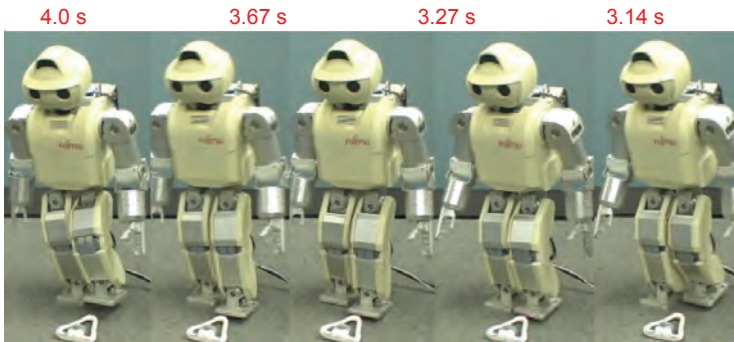


Fig. 27. Adaptive reflex against sudden obstacle under similar conditions of that in Fig. 10; the ankle of the left leg is pitched at the detection time of the obstacle, then it is controlled

such that the center of pressure is in the middle of the sole plate. At the same time the leg is extended so that the state of the robot reaches the equilibrium point under the right leg.

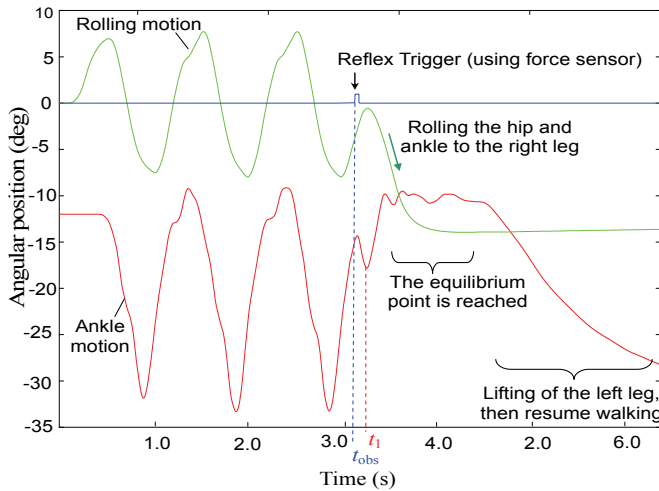


Fig. 28. Ankle joints' outputs when the proposed reflex against sudden obstacle is activated

At 3.14 s, the sole sensor of the left leg touches the obstacle and the pitching joint of the ankle was controlled according to (24) by $s_a(t)$ (fast response), then by $r_a(t)$ at 3.27 s, which is delayed by $1/a_{ii}$. Fig. 29 shows the ZMP position, where the location of obstacle is as described in Fig. 23a. The state of the robot reached the equilibrium point at about 4.0s, where the rolling joints get the static value (the projection of COM is under the right leg). Notice that the mode to resume motion by walking on obstacle is still under research.

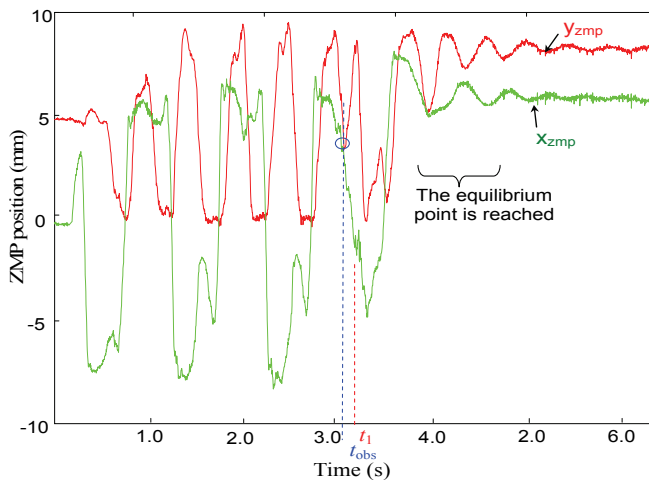


Fig. 29. ZMP position when reflex against sudden obstacle is activated

5. Conclusion

The reflex system was combined with the motion pattern generator to improve the robustness against lateral and frontal disturbances. On the other hand, the reflexes that highly adapt and control the movement of the humanoid in the presence of large disturbance acting on the robot's upper body were considered in a unified form. It was shown that a reflex movement was successfully enabled and integrated with the rhythmic motion in the cases of a sudden change in the floor level and a sudden obstacle, and in the presence of a large disturbance. Moreover, the proposed reflex against sudden obstacle was further investigated, and it was shown that when obstacle collides with the sole plate of the robot leg in a location out of a defined stable domain, the robot could not reach stability and fall down. On the other hand, an adaptive reflex was proposed that consisted of increasing the support polygon by controlling the ankle joint of the leg touching the obstacle. In order to demonstrate the effectiveness of the proposed system, we used the humanoid robot HOAP-3 of Fujitsu. It was shown that a reflex movement was successfully enabled and integrated with the rhythmic motion. As a future work, we will extend the reflex system by considering the interaction between the upper and lower body of the humanoid robots.

6. References

- Fujitsu Automation. <http://jp.fujitsu.com/group/automation/en/>
- Gerstner, W. (1995). Time structure of the activity in neural network models, *Phys. E.* 51, pp.738-758, *Rev*, 1995
- Grillner, S. (1985). Neurobiological bases of rhythmic motor acts in vertebrates, *Science*, no. 228, pp143-149, 1985
- Huang, Q.; & Nakamura, Y. (2005). Sensory Reflex Control for Humanoid Walking, *IEEE Trans. Robotics and Automation*, vol. 21, no.5, pp. 977-984, Oct. 2005
- Huang, Q.; Yokoi, K.; Kajita, S.; Kaneko, K.; Koyachi, N.; Arai, H.; & Tanie, K. (2001). Planning walking patterns for a biped robot, *IEEE Trans. Robotics and Automation*, vol. 17, no. 3, pp. 280-289, Jun 2001
- Kajita, S.; & Matsumoto, O. (2001). Real-time 3D walking pattern generation for a biped robot with telescopic legs, *Proceeding of the IEEE International Conference on Robotics & Automation*, pp.2299-2306, 2001
- Khalil, H. (1996). *Nonlinear Systems*, Printice Hall, ISBN 0-13-067389-7, New York
- Miura, H., & Shimoyama, I. (1984). Dynamic walk of a biped, *The International Journal of Robotics Research*, vol. 3 no. 2, pp.60-74, 1984
- Morisawa, M.; Kajita, S.; Harada, K.; & Fujiwara, K. Emergency Stop Algorithm for Walking Humanoid Robots, *IEEE/RSJ International Conference on Intelligent Robots and Systems*, pp. 2109- 2115, 2005
- Murase, Y.; Yasukawa, Y.; Sakai, K.; & Ueki, M.(2001). Design of Compact Humanoid Robot as a Platform", *19th Annual Conf. of the Robotics Society of Japan*, pp.789-790, 2001
- Okada, M.; Osato, K.; & Nakamura, Y. (2005). Motion Emergency of Humanoid Robots by an Attractor Design of a Nonlinear Dynamics, *IEEE International Conference on Robotics and Automation*, pp. 18- 23, 2005
- Taga, G. (1995). A model of the neuro-musculo-skeletal system for human locomotion, I. Emergence of basic gait, *Boil. Cybern*, no.73, pp.97-111. 1995

- Taga, G.; Yamaguchi, Y.; & Shimizu, H. (1991). Self organized control of bipedal locomotion by neural oscillators in unpredictable environment, *Biological Cybernetics*, vol. 65, pp.147-159, 1991
- Vukobratovic, M.; & Juricic, D. (1969). Contribution to the Synthesis of Biped Gait, *IEEE Trans. On Biomedical engineering*, vol BME-16, No. 1, pp. 1-6, 1969
- Zaier, R. & Nagashima, F. (2004). Motion Generation of Humanoid Robot based on Polynomials Generated by Recurrent Neural Network, *Proceedings of the First Asia International Symposium on Mechatronics*, p.659-664, 2004
- Zaier, R.; & Nagashima, F. (2006). Motion Pattern Generator and Reflex System for Humanoid Robots, *Proceeding of IEEE/RSJ International Conference on Intelligent Robots and Systems*, 2006